
FINAL INFARCT PREDICTION IN ACUTE ISCHEMIC STROKE

INTRODUCING STROKE, THE CORE-PENUMBRA CONCEPT AND MACHINE LEARNING APPLICATIONS

✉ **Jeroen Bertels**

Processing Speech and Images
Department of Electrical Engineering
KU Leuven, Belgium
jeroen.bertels@kuleuven.be

David Robben

Processing Speech and Images
Department of Electrical Engineering
KU Leuven, Belgium
david.robbe@kuleuven.be

Dirk Vandermeulen

Processing Speech and Images
Department of Electrical Engineering
KU Leuven, Belgium
dirk.vandermeulen@kuleuven.be

Robin Lemmens

Laboratory of Neurobiology
Department of Neurosciences
KU Leuven, Belgium
robin.lemmens@kuleuven.be

ABSTRACT

This article focuses on the control center of each human body: the brain. We will point out the pivotal role of the cerebral vasculature and how its complex mechanisms may vary between subjects. We then emphasize a specific acute pathological state, i.e., acute ischemic stroke, and show how medical imaging and its analysis can be used to define the treatment. We show how the core-penumbra concept is used in practice using mismatch criteria and how machine learning can be used to make predictions of the final infarct, either via deconvolution or convolutional neural networks.

Keywords Acute Ischemic Stroke · Core and Penumbra · Medical Imaging · Machine learning · Deconvolution · Convolutional Neural Networks

1 The cerebral vasculature

On average, the human brain accounts for about 20 % of the total energy consumption and a similar fraction of the total cardiac output of an adult at rest, while the brain represents only about 2 % of the whole body size [76, 55]. Unable to store energy and relying almost exclusively on the aerobic consumption of glucose, a constant functioning of the cerebral vasculature is paramount to carry oxygenated, glucose-rich blood throughout the brain parenchyma to every single cell.

From a hemodynamics standpoint, and under the assumption of having an adequate blood composition in the feeding arteries to the brain, parenchymal access to oxygen and glucose can be described by two time-dependent parameters: the cerebral blood flow (CBF) and the cerebral blood volume (CBV), i.e., the flow rate through (ml/100 g/min) and volume of blood in (ml/100 g) a certain piece of tissue, respectively. As such, the correct and continuous functioning of brain cells depends on the constant tuning of CBF and CBV at each location, keeping them within the functional range. Healthy values of CBF and CBV may shift slightly across subjects, and are different in gray matter (around 80 ml/100 g/min and 4 ml/100 g) and white matter (around 20 ml/100 g/min and 2 ml/100 g) [94, 16]. The brain has developed anatomical and functional features to combat various pathological vascular conditions that would influence those variables [68].

1.1 Anatomy

The first line of defense lies in the anatomical structure of the cerebral vasculature (Figure 1). Three large arteries feed oxygenated, glucose-rich blood to the brain, while two large veins drain deoxygenated, glucose-deprived blood from the brain. Inside the brain, these vessels form diverging and converging branches, respectively, and connect at the level of the capillaries, where eventually, the extracellular fluid mediates the exchange to and from the cells. Due to the

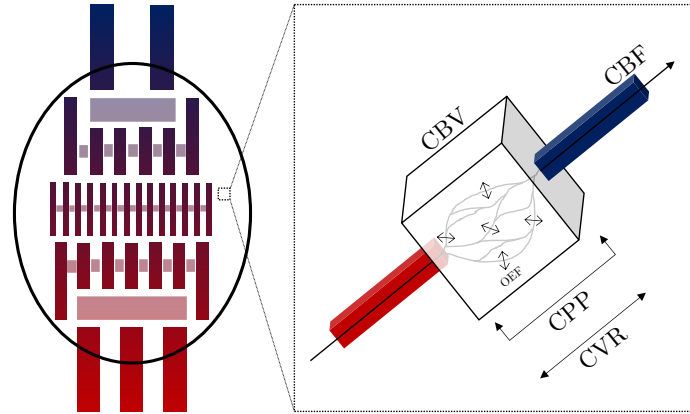


Figure 1: The cerebral vasculature. LEFT: A schematic representation of the cerebrovascular anatomy. Arterial and venous trees connect at the level of the capillaries, respectively carrying oxygen- and glucose-rich (RED) and -deprived (BLUE) blood. Transparent lateral connections refer to the collateral circulation, less or more pronounced across different subjects. RIGHT: A piece of tissue contains many capillaries and cells. Blood perfusion takes place when the CPP overcomes the CVR. A combination of the CBF, CBV and OEF summarizes the access to oxygen and glucose.

well-developed collateral circulation, i.e., blood may follow different trajectories to reach a certain destination, CBF and CBV may be well preserved across the entire brain even in the case of an abrupt and local structural change. This way, the communication between the three feeding arteries at the circle of Willis is of crucial importance [87]. Other significant collaterals exist, e.g., through anastomoses between the external carotid artery branches and the intracerebral circulation and between vessels at the surface of the brain [104]. Nonetheless, some brain regions are particularly vulnerable, e.g., regions at the boundaries between the anterior, middle, and posterior cerebral arteries and territories supplied by end arteries [68].

1.2 Autoregulation

As a second line of defense, nature has equipped the brain with the functional phenomenon of cerebral autoregulation. Under normal conditions, there is a direct relationship between CBF and CBV. The cardiac system maintains a negative pressure gradient, i.e. cerebral perfusion pressure (CPP), across the brain from arterial input to venous output, enough to overcome the cerebrovascular resistance (CVR) and reaching sufficient CBF at each location (Figure 1). When the small intracranial vessels (the predominant resistance vessels) constrict or dilate, the CVR increases or decreases, respectively, and the CBV and CBF would both decrease or increase until new steady-state conditions are obtained. Via active or passive mechanisms of vasoconstriction and -dilation, CBF remains relatively constant despite moderate variations in CPP.

1.3 Other mechanisms

To compensate for additional hemodynamic changes, brain parenchyma can also alter its own state and increase or decrease the oxygen extraction fraction (OEF) from blood [68] (Figure 1). Numerous studies have shown that a local increase in neuronal activity results in a local increase in glucose utilization, accompanied by local increases in CBF [90]. Changes in blood O_2 and CO_2 concentrations act through direct and indirect effects. In conditions of hypoxia or hypercapnia, via concomitant changes in the pH of brain tissue, CBF is altered directly by changing the CVR or indirectly through the release of vasoactive factors [76].

1.4 Intra- and inter-subject variability

The state and capacity of these defense mechanisms vary widely across subjects. Although we all share the basic cerebrovascular anatomy, collateral circulation can be more or less pronounced [59]. Even under normal operating conditions, the lower and upper limits of cerebral autoregulation are not fixed. As such, the exact values of both CBF and CBV may vary due to various physiological variables, including arterial blood gases (e.g. NO is an important mediator controlling basal CBF [109, 110]) and metabolic rate through vasoneuronal coupling (e.g. an upward shift of both limits due to sympathetic activation to anticipate an increase in CPP [68]). Similarly, certain disease states result in a prolonged shift (e.g., an upward shift of the autoregulatory plateau in patients with chronic hypertension [96]).

2 Acute ischemic stroke

Despite these mechanisms, there are pathological states of what is called cerebral *ischemia* in which the CBF and CBV are insufficient to meet the metabolic demand. A chronic fall in CBF can happen, e.g., under systemic arterial hypotension or severe stenosis in one of the feeding intra- or extracranial arteries. However, before the cerebral metabolic rate of oxygen begins to fall, the OEF increases as a fallback mechanism. Therefore, it is primarily an acute change in the cerebral vasculature that pushes the CBF abruptly outside its operating range, albeit more likely in subjects with preliminary chronic changes and limited collateral circulation.

2.1 Neuronal dysfunction

In severe focal ischemia, the CBF starts to decrease passively with any further decrease in CPP. From that point we can identify critical CBF thresholds at which certain neuronal functions are lost [47] (Figure 2). This pattern of thresholds is complex, and the exact levels vary with the duration of the event and across different animal models. Generally, the first thresholds ($\pm 80\text{-}40$ ml/100 g/min) relate to a decline in protein synthesis, selective gene expression, and selective neuronal loss. A more progressive breach ($\pm 40\text{-}15$ ml/100 g/min) results in the loss of electrical function, transpiring into clinical symptoms. The sudden onset of symptoms of neurological deficit of presumed vascular origin results in the clinical diagnosis of stroke. Two main types of stroke can be defined based on the acute cause of the ischemia: an ischemic stroke ($\pm 80\%$) and a hemorrhagic stroke ($\pm 15\%$). In an acute ischemic stroke (AIS), the ischemia is attributed to the occlusion of an artery (e.g. as a result of an embolism originating from the heart). In a hemorrhagic stroke, an artery is ruptured, resulting in the acute accumulation of blood within the brain parenchyma. Often, the classification includes a third type: a transient ischemic attack ($\pm 5\%$). A transient ischemic attack is similar to an AIS, but as its name suggests, the ischemia is only temporary and does not cause permanent damage [21]. The effects and potential treatments may differ between ischemic and hemorrhagic stroke. Nonetheless, they share a similar symptomatic pattern and progression of the parenchymal tissue under ischemia. From now on, the focus is on AIS, more specifically following a large vessel occlusion in the anterior circulation.

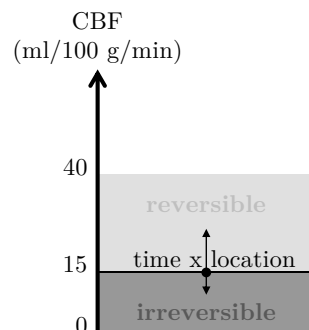


Figure 2: During a pathological state of cerebral perfusion, the CBF decreases progressively. It turns out that CBF levels correlate with irreversible and reversible tissue damage. Nevertheless, absolute thresholds vary across different subjects, and with time and location due to a complex cascade of cellular reactions.

2.2 Core and penumbra

When the CBF decreases to the lowest regions ($\pm 15\text{-}0$ ml/100 g/min) a loss of cellular ion hemostasis occurs [47, 106]. While the clinical symptoms are similar, brain tissue will typically undergo irreversible tissue damage and become *infarcted*, i.e., the *core* of the ischemic tissue. With the introduction of irreversible tissue damage, we have implicitly introduced reversible changes for higher levels of CBF, thus brain tissue that may recover when the blood perfusion is restored, i.e., the *penumbra* of the ischemic tissue. However, this whole concept of irreversible versus reversible, core versus penumbra, and non-salvageable versus salvageable, is highly complex and is still the subject of ongoing research. What is certain is that there is no one-to-one relationship with the absolute value of the CBF, not across different subjects nor within a single subject. For an intuitive elaboration of what would happen when blood flow is restored, thus what part of the brain can be salvaged, we need to introduce at least two additional variables: time and location (Figure 2).

2.2.1 Time

Imagine that the immediate opening of the vessel follows the abrupt occlusion. In this case, tissue may recover completely, despite local, short-term levels of detrimental CBF. Per definition, non-salvageable and salvageable tissue can only be defined at a certain moment after stroke onset (Figure 3). In fact, the concept that neuronal survival depends on the time since onset (TsO) dates back from 1981 [4, 42, 52]. From here a continuum emerged of neurons surviving indefinitely with a CBF above 15 ml/100 g/min but dying within 30 min with a CBF below 10 ml/100 g/min. In non-human primates, for instance, brain ischemia of 10 to 15 ml/100 g/min can sustain for 2 to 3 hours without irreversible injury. This “time is brain” relationship has a deep-rooted foundation in early clinical trials, which do patient triage based on the TsO [69, 37]. Since these treatments aim to restore blood perfusion, this implicitly states that the amount of salvageable tissue decreases over time and thus that the core eats away the penumbra.

2.2.2 Location

In a way, the fact that an increasing TsO results in a virtual, upward shift of the lowest CBF region at a particular location can be attributed to the status of the neighboring parenchyma. This spatial dimension arises since a complex cascade of biochemical processes lies at the origin of cellular breakdown. With a progressive decrease in CBF across the

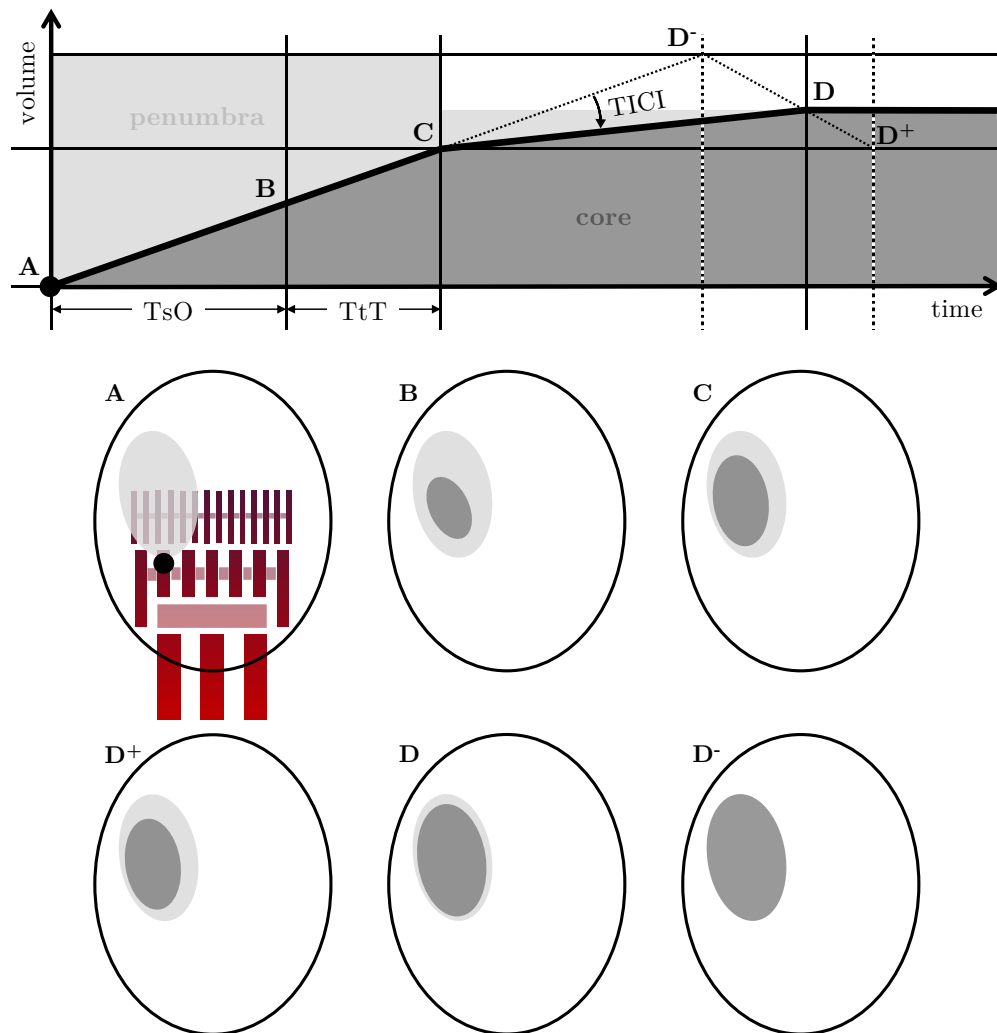


Figure 3: At the onset of an AIS there is no irreversible damage (A). After a certain TsO, the patient is triaged for a certain treatment, a.o. based on acute imaging and estimates of the tissue state (i) at that moment (B), and (ii) at the moment when the (partial) reperfusion takes place, i.e. after a certain TtT (C). The treatment affects the extent of the final infarction ($D^- > D > D^+$) and may slow down the progression (decreasing the tissue hypoperfusion will suppress its malicious effect on surrounding tissue). To assess the final infarction, follow-up imaging should be acquired not sooner than when the infarction has fully progressed (D^+).

critical levels, the increase in anaerobic energy metabolism results in acidosis with an increase in lactate and glutamate. Eventually, neuronal cells will undergo a generalized collapse of membrane function with anoxic depolarisation due to unbalanced in- and efflux of cellular ions. It has been shown that this malign environment can spread out, e.g., via peri-infarct depolarizations [48], diffusion of glutamate [17] or inflammation-related processes [105].

2.3 Treatment

At a certain point, the entire penumbra will turn into core (Figure 3). As discussed before, the time this takes and the final volume vary widely across patients. Any intermediate external intervention that leads to increased blood perfusion can be considered a potential treatment. In practice, there are two established reperfusion therapies for an AIS: via the administration of drugs (i.e. intravenous treatment (IVT) [69]) or via mechanical recanalization (i.e. thrombectomy or intra-arterial treatment (IAT) [37]). Care should be taken to avoid distal microvascular obstruction, which would further contribute to the progression of the ischaemic damage [23]. Different approaches to quantifying the effect of treatment are possible. Straightforwardly, the direct effect on blood perfusion can be quantified by the modified Thrombolysis in Cerebral Infarction (mTICI) score [45]. The higher the mTICI score ($mTICI \in [0, 1, 2a, 2b, 2c, 3]$), the better the recanalization (potentially the reperfusion) and the slower the further progression of the infarct (Figure 3). Additionally, it is important for this effect to take place soon after hospitalization and when the decision on the treatment was made, i.e., the time to treatment (TtT) (Figure 3). Success also means avoiding adverse effects such as bleeding, cerebral swelling, or damage to the inner arterial lining (which happens during IAT). Other quantifiers correlate indirectly with the amount of reperfusion but aim to score a patient's well-being days or months after the event. As such, the National Institute of Health Stroke Scale score (NIHSS) measures the neurological deficit by scoring the specific ability on 11 items. The higher the NIHSS score ($NIHSS \in [0, 42]$), the larger the impairment. The modified Rankin Scale (mRS) score measures the degree of disability or dependence in daily activities. The larger the mRS score ($mRS \in [0, 6]$), the larger the disability, with 0 having no symptoms and 6 indicating dead. The mRS has become the most widely used clinical outcome measure for evaluating potential stroke therapies in clinical trials.

3 The role of imaging

The likelihood of recovery to independence after AIS is significantly improved by reperfusion, either by IVT or IAT. However, the marginal correlation between mTICI and mRS is weak due to the highly complex interaction between subject, time, location, and treatment. There are certain scenarios in which treatment should be avoided. In general, this treatment decision depends on balancing the possibility of a good clinical outcome against the risk of complications. Complications of IVT include intracranial hemorrhage (ICH), systemic bleeding and orolingual oedema [29, 99]. Complications of IAT also include ICH, but are mostly related to radiological contrast media and device-related vascular injury [99]. The risk of ICH is directly related to the ischemia status since oxygen and glucose are also needed to maintain the structural integrity of the vessels. Therefore, the absolute estimation of core and penumbra volumes at the time of triage and the time of estimated reperfusion becomes the key ingredient for making a well-considered decision (Figure 3). It is for this purpose that acute imaging is used.

3.1 Acute imaging

Two complementary imaging approaches can be classified based on the direct or indirect nature of estimating the underlying parenchymal tissue status. Direct methods rely on the fact that the underlying biochemical cascade changes the measured signal of a particular imaging modality at the voxel level. Indirect methods do this via the offline measurement of blood perfusion dynamics from a series of direct image measures at the voxel level. Due to partial volume effects, the measured voxel value represents a sort of average of the underlying mechanisms and interactions that are taking place between the tissue and the imaging signal, which is then captured by the imaging detector and finally reconstructed as a voxelized image. In practice, the voxel size could be 1 mm x 1 mm x 1 mm, defined as a compromise between image noise, resolution, and acquisition time. If we consider the tuboid shown in Figure 1 to represent a single voxel of that size, it could be a network of hundreds of capillaries and thousands of cells, potentially from multiple capillary beds, fed and drained by different arterioles and venules, respectively.

3.1.1 Direct imaging

Via the extensive histological study of the evolution of ischemia in animal models, it became clear that early molecular changes, corresponding to the higher CBF threshold levels and even selective neuronal necrosis, are unlikely to be detected by practical imaging methods [32, 30, 31, 33, 34, 35]. A better imaging biomarker is ischemic edema, i.e., monitoring the intra- and extra-cellular water content. It turns out that the complex cascade of cellular breakdown, as soon as there is energy depletion, goes hand in hand with different types of ischemic edema [95, 106]. First, cytotoxic

or cellular edema results in the redistribution of ions and water from the extra- to the intra-cellular environment (starting from CBF values below ± 30 ml/100 g/min [49]). Then, when there is (minimal) perfusion and an intact blood-brain-barrier, ionic edema results in both the redistribution of ions and water from the intra-vascular to the extra-cellular environment and the net increase of tissue water content (starting from CBF values below ± 20 ml/100 g/min [97]), compensating for changes induced by the cytotoxic edema. The ionic edema itself may further decrease the CBF, and depending on the exact level and duration of the event, lead to irreversible changes within a timespan of 60 min [51, 103]. Finally, vasogenic edema results in a further net increase of tissue water content due to blood-brain-barrier failure, followed by leakage of plasma proteins. This will result in hydrostatic and osmotic pressure gradients, causing severe brain tissue swelling, mass effects, and a further reduction in CPP, resulting in irreversible damage. Yet again, care must be taken with timing and absolute CBF levels due to the complex interplay between time and location.

NCCT In one voxel, the overall attenuation coefficient for X-rays will only change as soon as there is a net increase in tissue water content. As a result, it is evident, and confirmed with experimental and clinical observations [106], that plain computed tomography (CT), i.e. non-enhanced or non-contrast CT (NCCT), can detect ionic brain edema and as such irreversible ischemia. However, early ionic changes, with an increase in tissue water content of less than 1 %, result in subtle hypoattenuation, especially in gray matter. Expert knowledge is required, and considerable inter-rater variability remains in voxel-based analysis. In an attempt to quantify the CT hypoattenuation, and thus ionic edema, within the MCA territory, the Alberta Stroke Program Early CT Score (ASPECTS) was introduced [6, 85]. The lower the ASPECTS (ASPECTS $\in [0, 10]$), the more regions are included in the segmental estimate of the infarct, with 10 indicating no regions and 0 indicating all 10 predefined regions involved.

MRI Frequently used MRI sequences for AIS imaging fall under the term of diffusion-weighted imaging (DWI), in which the diffusion of water molecules interacts with the imaging signal and creates contrast. Since cytotoxic edema is associated with diffusion impairment, it will lead to hyperintensity on DWI. For quantification purposes, the apparent diffusion coefficient (ADC) in each voxel, mainly influenced by Brownian motion, can be calculated from DWI values at different settings. Indeed, it has been shown that ADC values decrease as soon as CBF drops below 20-40 ml/100 g/min, on its turn related to shrinkage of extracellular space [61, 107, 49].

3.1.2 Indirect imaging

As discussed, blood perfusion dynamics, such as CBF, greatly influences the tissue status. Indirect methods, therefore, aim to capture these dynamics on the voxel level and relate this to reversible or irreversible damage.

CTP and PWI The idea is simple: after the intravenous injection of a contrast agent at t_0 a series of 3D images, acquired between t_s and t_e , show the passage of contrast through the brain (Figure 4). For this purpose, either CT perfusion (CTP) or perfusion-weighted imaging (PWI) can be used, respectively using CT and MRI imaging to capture the change of contrast inside a piece of tissue (remember the cuboid from Figure 1) as a change in image intensity, on its turn converted into a change in concentration of the contrast agent over time, i.e. the time concentration curve (TCC). Nevertheless, even for a piece of “tissue” fully inside a vessel, the TCC will flatten along its trajectory in the vessel due to laminar flow and diffusion. Depending on the exact situation (e.g., the injection protocol itself, a patient’s cardiovascular

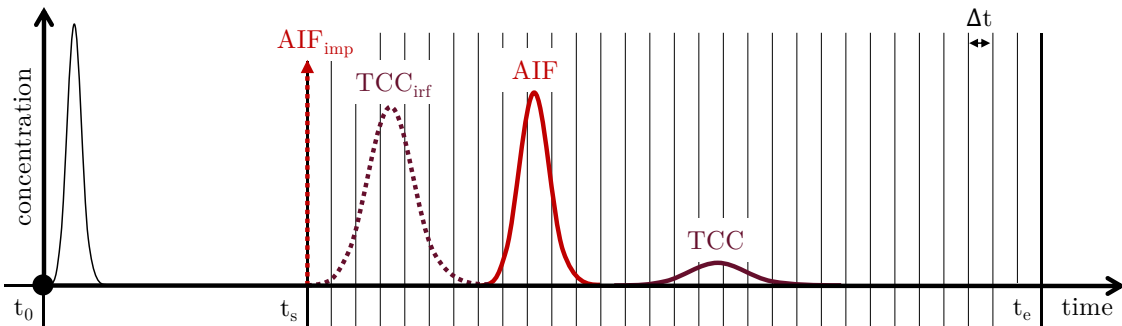


Figure 4: Perfusion imaging acquires a series of images between t_s and t_e after the injection of a contrast agent at t_0 . The measured TCCs will look different across different patients and measurements, even so for the injection location itself and for the location of the AIF at the entrance of the brain. Measurements can be normalized, i.e. TCC_{irf} , by deconvolution, as if they were the result of an AIF_{imp} . Straightforwardly, the timing of the start $t_s - t_0$ and end $t_e - t_0$ of the scan is of crucial importance. The time resolution Δt is important for the deconvolution to be mathematically valid. From the resulting TCC_{irf} s certain perfusion dynamics can be derived directly.

system, motion), the TCCs will look different across different patients and multiple measurements. In theory, it is possible to normalize cerebral TCC measurements as if they were all the result of an identical TCC at the input of the brain, i.e., the arterial input function (AIF). Deconvolving the measured TCCs with the measured AIF normalizes the AIF to be the Dirac impulse (AIF_{imp}) and normalizes the TCCs to be the tissue's impulse response functions (TCC_{inf}). It turns out that, under reasonable assumptions (e.g., the contrast agent stays within the vessels), this deconvolution strategy is indeed valid and that from the TCC_{inf} certain perfusion dynamics can be derived straightforwardly.

PET and SPECT In contrast to the endogenous character of CTP and PWI, nuclear medicine methods use exogenous radionuclides as tracers. In both single photon emission CT SPECT and positron emission tomography PET the accumulation and decumulation of these tracers inside the tissue can be measured, from which the blood perfusion dynamics can be derived [119]. The fully quantitative nature of PET further allows the measurement of the OEF. Currently, PET and SPECT are used less frequently compared to CTP and PWI in the acute clinical setting. Nonetheless, they deserve mentioning due to their early contribution to pathophysiological research on irreversible versus reversible tissue damage following an AIS [7, 8, 113, 67].

3.1.3 Other imaging

Besides imaging that tries to estimate tissue status on a voxel basis, additional imaging is needed to triage patients correctly because IAT requires mechanical recanalization, which limits its application to proximal thrombi.

CTA and MRA CT angiography (CTA) or MRI angiography (MRA) aims to visualize the vasculature in the entire head and neck region with sufficient resolution, primarily to assess the exact location of the occlusion and its mechanical accessibility to effectively perform IAT. The acquisition is similar to CTP and PWI, with the machine parameters and contrast injection tuned to obtain a superior axial extent and image quality at the expense of acquiring only a single 3D volume. Despite its primary objective, CTA or MRA is also used to assess collateral circulation (CC) scores in a qualitative manner. For example, the degree of pial or leptomeningeal CC in AIS has been associated with infarct volume, ICH and mRS [59, 20, 5, 66, 98]. More recently, multi-phase CTA or MRA is used, e.g., to visualize the vasculature during early-arterial, late-arterial, and venous passage of contrast agent. In this perspective, multi-phase CTA may improve CC evaluation, showing superior inter-rater agreement and clinical outcome prediction [74, 73, 78]. More recently, it has been shown that IAT is effective after CC score-based patient selection [36] and that CC scores can independently predict the progression of middle cerebral artery infarct [28].

CTP versus CTA Technical limitations in modern CT, such as the rotation speed ($\pm 360^\circ/s$) and axial detector size (4-16 cm), result in a trade-off between the temporal resolution and the axial extent. Detector movements in the axial direction, via helical or jog-mode scanning protocols, increase the axial extent at the cost of temporal resolution and additional processing (e.g., motion correction, different axial positions have different timings). Furthermore, multiple acquisitions at a certain axial position increase radiation dose. Following the “as low as reasonably possible” principle, this further adds the tube-load and the total number of acquisitions to the trade-off. The combination of (i) a practical CTP iodine contrast injection protocol (5-6 ml/s for a duration of 5-6 s), (ii) variations in the cardiovascular dynamics taking place between the injection site and the brain inlet, and (iii) variations in cerebral perfusion dynamics, demand a CTP duration t_e-t_s of about 1 min (Figure 4). Recent research also investigated the effects of varying the temporal resolution and tube load on the diagnostic quality of CTP-derived perfusion dynamics [50]. The lowest possible dose protocol was set at $\Delta t = 2$ s and a tube load of 100 mAs, which limits the axial extent of current CTP to 8-32 cm as observed in clinical practice. Given these variables, CTA is nothing more than a specific CTP setting with (i) a wider injection bolus (± 3 ml/s for a duration of ± 25 s), (ii) $\Delta t = t_e-t_s$ and (iii) t_e-t_s such that the entire head and neck region is captured (Figure 4). Since the reconstruction of a single rotation averages the underlying dynamics of the contrast agent over the rotation period, the exact setting is defined such that the maximum of any vascular TCC plateaus over the entire scan duration. It has been suggested that multi-phase CTA could substitute the diagnostic value of CTP. Though this might be true from a pure diagnostic standpoint, in the limit CTP contains (multi-phase) CTA, while exact blood perfusion dynamics can only be obtained using higher temporal sampling rates.

3.2 Follow-up imaging

Follow-up imaging aims to reassess the state of the cerebral tissue and check if the treatment was successful. Especially in the case of IVT, guidelines recommend a follow-up CT or MRI scan after 24 h to exclude ICH and decide on the initiation of a secondary preventive treatment with antithrombotic agents [84]. In general, without any secondary reperfusion treatment, follow-up imaging should be able to indicate the final infarct. As a result, this type of follow-up imaging should be acquired no sooner than when the infarct has fully progressed (Figure 3). Typical timing is between

24 h and 5 days. The type of imaging can be similar to the acute phase, mostly direct since the more pronounced edema can now be detected with higher sensitivities.

4 Final infarct prediction

Estimates of core and penumbra volumes can be seen as imaging biomarkers. Integrated with clinical information of the patient (e.g. age, stroke history, drugs), an estimated TtT and mTICI score, they form a holistic basis to triage AIS patients. For this purpose, recent research and trials focus on the quantitative and voxel-based estimation of core and penumbra using data-driven methods.

4.1 Data-driven core and penumbra estimation

Data-driven methods use machine learning to learn a mapping from input to output (Figure 5). This mapping is accomplished by a certain model, which contains a number of parameters that are tuned such that the mapping is optimal on a known dataset of input-output pairs. During optimization, the difference between a ground truth (e.g. manual) output and its prediction, i.e. the “loss”, is minimized by iterating across all input-output pairs in the dataset until convergence. State-of-the-art methods aim to produce segmentation maps, e.g. one for the core and one for the penumbra. Before digging into the current benchmark, we will describe briefly two fundamental aspects regarding the core and penumbra terminology.

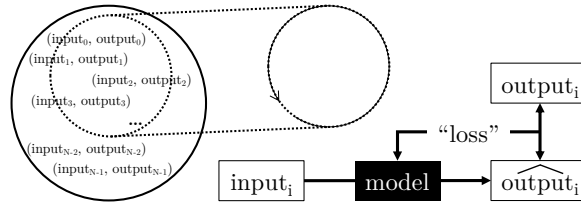


Figure 5: Data-driven methods for automated tissue status segmentation in AIS need (i) a dataset of input-output pairs, and (ii) a model that maps an input to an output. The model has trainable parameters that are tuned (iteratively) to minimize the loss between the observed and predicted output. Current methods mostly provide models for different subsets of the original dataset, e.g. one for core and one for penumbra estimation, respectively using a dataset of reperusers and non-reperusers.

4.1.1 Ground truth generation

While the idea to learn a data-driven mapping is simple, it raises the question of how to obtain valid datasets of input-output pairs for the tasks of core and penumbra estimation. Following Section 3, it is expected that the core and the penumbra can be deduced from acute NCCT and DWI imaging, respectively. However, there are two limitations to their effective use. First, in clinical practice the concurrent acquisition of both modalities is rare, and most often a sole CT-based workup is done due to various reasons, including availability, safety, and speed. Second, the exact mapping from CT or ADC values to irreversible or reversible changes, respectively, is non-trivial. Therefore, from a theoretical point of view, follow-up imaging, either CT- or MRI-based, is the gold standard. In fact, by using follow-up imaging we construct a database in which the output represents the follow-up, i.e. final, infarcts. In the limits, in some subjects the final core will be equal to the acute core, i.e. the core at the time of acute imaging, in others it will represent the acute core plus penumbra ($core \cup penumbra$). Respectively, these groups are often called reperusers and non-reperusers, thus reflecting subjects with instantaneous complete reperfusion at the time of acute imaging and subjects in whom no (partial) reperfusion was achieved until follow-up.

4.1.2 Ambiguities in their definition

Up till now, we followed the definition of core and penumbra as being, at a certain point in time, irreversibly and reversibly damaged, and thus non-salvageable and salvageable tissue, respectively. From a practical point of view, it is impossible to construct a database as described before for acute core estimation since it is impossible to obtain complete recanalization at the exact time of the acute imaging, i.e. there will always be a certain $TtT > 0$. Similarly, the description of the penumbra becomes ambiguous, while the $core \cup penumbra$ remains exact. This discrepancy has led to a secondary interpretation of their definition: core and penumbra as being the estimated irreversibly and reversibly damaged tissue at the time of recanalization [38]. In other words, a medical doctor often reasons in terms of “What can we still save?”, inherently taking into account a significant TtT. Potentially, this has led to a misinterpretation of the value of DWI, which is generally accepted as the gold standard to identify the core, and thus irreversibly damaged

tissue. However, this is only true as far as it concerns the estimation under current constraints, and as such, care must be taken when interpreting the acute DWI. For example, if DWI is (partly) sensitive to the penumbra, it could be the modality of choice to estimate follow-up infarct volumes when $Tt > 0$.

4.1.3 The present: DCV-based estimation

Most data-driven methods to estimate core and penumbra in clinical practice use indirect imaging, more specifically perfusion imaging. In fact, via DCV, perfusion measurements can be normalized and quantified across different subjects and acquisitions, and the resulting TCC_{irf} s contain direct information on the blood perfusion dynamics of the underlying parenchymal tissue [27]. For example T_{max} and CBF maps can be derived from the TCC_{irf} map as:

$$T_{\text{max}} = \arg \max_t TCC_{\text{irf}}, \quad (1)$$

$$CBF \propto \max_t TCC_{\text{irf}}. \quad (2)$$

After dichotomization into input-output datasets of reperfusers and non-reperfusers, the typical strategy is to find the optimal combination of perfusion parameter and threshold with respect to volume estimation of the follow-up infarct [111, 11]. It turns out that the follow-up infarct volume of reperfusers and non-reperfusers, and thus the acute core and core \cup penumbra is best approximated with:

$$\text{core} \cup \text{penumbra} \approx T_{\text{max}} \geq 6 \text{ s}; \quad (3)$$

$$\text{core} \approx rCBF < 0.30, \quad (4)$$

as in [81] and [14], respectively. Note that instead of the CBF the relative CBF (rCBF) is used, in which the CBF values are relative to normal white matter. The use of T_{max} and rCBF to obtain core and penumbra estimates can be considered the current benchmark. Nevertheless, alternative perfusion maps and thresholds exist, e.g. using the relative CBV (rCBV) and delay time (i.e., the T_{max} after delay-corrected perfusion analysis), respectively $rCBV < 0.60$ [18] and a delay time < 3 s [60] for core and core \cup penumbra. While the core is often estimated using DWI, the core \cup penumbra is mostly estimated using perfusion imaging, hence the name perfusion lesion.

4.2 Triage in clinical practice

The importance of the imaging-based selection of patients that would benefit from acute reperfusion therapy grows rapidly [93]. Nevertheless, their effective use to triage AIS patients is fairly new. In fact, clinical practices often still use qualitative proxies of tissue status derived from NCCT or MRI [82] in combination with TsO windows. Luckily, the ongoing quest to select patients more carefully, both inside and outside these TsO windows, has led to the incorporation of so-called mismatch criteria into current clinical practice.

4.2.1 Qualitative proxies and TsO

Back in 1995, IVT became the first internationally approved treatment for eligible AIS patients, at least when it could be administered within a $TsO < 3$ h [69]. It is only in 2008 that its efficacy and safety could be established in the extended time window of $TsO < 4.5$ h, in part due to the first (qualitative) imaging-based exclusion criteria, being a visible indication that $> 1/3$ of the MCA was affected [40]. Similarly, in the triage for IVT an ASPECTS < 7 was often used as contra-indication. This roughly relates to core estimation: the more irreversibly damaged tissue, the higher the risk for developing symptomatic ICH when blood perfusion would be restored. In addition, clinical deficit, e.g. in terms of the NIHSS score, could help to make a rough estimate of the core \cup penumbra, and thus the potential benefits.

The clinical introduction of IAT dates back from 2015 when five trials (MR CLEAN [9], ESCAPE [36], REVASCAT [91], SWIFT PRIME [15] and EXTEND IA [53]) showed a strong advantageous treatment effect within a time window of $TsO < 6$ h in the HERMES meta analysis [37]. The triage for IAT became independent to the triage for IVT, and also incorporated rather simple and qualitative imaging-based exclusion criteria. In the triage of IAT, the exact role of these scores was not consistent. Some trials simply used an ASPECTS < 6 as contra-indication, mainly to reduce the risk for symptomatic ICH. Other trials used a multi-phase CTA-based CC score [36].

While this qualitative triaging system is simple, it remains questionable since (i) reversible and early changes are not visible on NCCT [106], (ii) those core and penumbra estimations are not quantitative, nor voxel-based, and thus inefficient for long-term or location-based analyses, and (iii) it is prone to significant inter-rater variability [26, 71]. In this respect, the automated scoring of ASPECTS on acute NCCT has been investigated [57, 41], and proved to be non-inferior to their manual counterparts when correlated with DWI-based follow-up infarct volumes [77, 43]. By design, it cancels inter-rater variability, however, it still does not provide information on the tissue status of each voxel.

4.2.2 Mismatch criteria

Unfortunately, even though IVT and IAT can be considered highly effective, the effect is mitigated by the low proportion of patients that eventually qualify for such treatments [1]. For a true patient-specific triage, TsO should be seen as

only one of many factors playing a role in lesion growth [114, 75, 118, 86]. For this purpose, present research extends the use of qualitative CT-based analysis with multi-modal biomarkers in the form of so-called mismatch criteria, i.e. how much does a lesion identified on one modality differ from a lesion identified on another modality (or even within the same modality), hence the name mismatch. A mismatch criterion is typically defined by a combination of the volumetric difference, the mismatch ratio and a constraint on one of the lesion volumes. It should be clear that an estimated core-penumbra mismatch can be obtained using different modalities, but all have the purpose to balance the risks and benefits of the treatment.

The DWI-PWI mismatch (i.e. difference > 10 ml, ratio > 1.2) was one of the first quantitative estimators to identify subgroups that were likely to benefit or to be harmed when administering IVT in the extended TsO window of $3 < \text{TsO} < 6$ h [3]. To a certain extent, the DWI-PWI mismatch was able to predict malignant mismatches, e.g. that would result in symptomatic ICH. Some criteria were used merely as a simple proxy for TsO when unknown (e.g. DWI-FLAIR [101]). More recently, either direct or meta-analyses from WAKE-UP [102], EXTEND [65] and ECASS-4: EXTEND [13] have shown positive treatment effects of IVT in the later or unknown TsO windows when either rCBF-Tmax (i.e. mismatch > 10-20 ml, ratio > 1.2, core < 70-100 ml) or DWI-FLAIR mismatch (visible mismatch, no FLAIR lesion) criteria were used [100]. Only few trials, e.g. THAWS [56], were unable to show this effect, potentially due to the use of lower-dose-IVT.

Likewise for IAT, DAWN [80] and DEFUSE 3 [2] explored the use of core-penumbra mismatch, respectively rCBF/DWI-NIHSS and DWI-PWI, in the unknown and later time window of TsO < 24 h. Both mismatches were able to show a positive treatment effect (mismatch > 15 ml, ratio > 1.8, core < 70 ml).

4.3 The (near) future: CNN-based estimation

It is clear that a quantitative and voxel-based estimation of tissue status can lead to superior patient triage, thereby avoiding the sole use of proxies such as TsO (if known) and other qualitative estimators as sole predictors of AIS progression. By doing so, the difference in AIS progression across patients would become part of the solution instead of presenting itself as an additional source of variation when analyzing treatment effects. Nevertheless, the DCV-based estimation benchmark in current clinical practice has some limitations. Also, in parallel, more recent data-driven methods have been developed that are potentially more suitable for the task.

4.3.1 Current limitations

The problem with DCV-based core and penumbra estimation is at least twofold. First, the method is generally considered significantly sensitive to noise [12, 72], which is intrinsically relevant in CTP. Both the relatively low temporal resolution and signal-to-noise ratio make the discrete DCV mathematically ill-posed and hungry for regularization. In practice, both regularization and noise reduction are needed in order to obtain physiologically meaningful results [27]. Furthermore, DCV depends on AIF selection, which is prone to inter-rater variability [88]. Research towards automated AIF detection often targets local AIFs, which would be better suited for the theoretical DCV model [63]. However, this further adds partial volume effects to the equation, which in turn thrives research towards (automated) venous output function integration with problems of its own [58].

Second, from Section 2 it was clear that voxel-wise perfusion parameters alone per definition do not contain the necessary information to derive tissue status. As a result, the optimal solution for a single-parameter threshold model is very much dataset-dependent. It is not surprising that the optimal thresholds for derived perfusion parameters show large variability across different research [11, 18]. Add to this the specific regularization, noise reduction and other preprocessing steps that typically vary across different vendors. So even when a fixed threshold is used for mismatch calculation, be careful, e.g. in [25] two software packages give differences of 23.6 ml and 15.8 ml for core and penumbra estimation, respectively.

4.3.2 Added value of CNNs

Given these limitations, a first attempt using a generalized linear model to replace the single-parameter thresholding and including both PWI and DWI imaging had only limited success [117]. Later, non-linear models and region-based features were added to [92]. Similarly, after dichotomization into reperusers and non-reperusers, the use of random forest classifiers in combination with a larger spatial context and multi-modal MRI provided a substantial improvement over predefined thresholds to predict the follow-up infarct, respectively core and penumbra [70]. In parallel, also research towards DCV-free parameter estimation remained popular [72], but yet again seemed to ignore the effect of infarct location on its surroundings.

Spatial context and model complexity The abrupt takeover of almost the entire computer vision field by CNNs, is no less true here. Following the ISLES 2017 challenge [112], which compared methods to predict the follow-up

infarct based on acute DWI and PWI, it was clear that CNN-based methods were simply performing superior. Despite most methods still relying on perfusion parameters at the input, the model now incorporated spatiality and complexity more naturally. For example, deep CNNs outperformed both shallower CNNs and generalized linear models using nine biomarkers derived from MRI [79]. To test if the model could learn the treatment effect of IVT they dichotomized the dataset correspondingly and two independent models were learnt. While most methods work purely voxel-based, some do implement additional shape space interpolation [64].

Most methods use perfusion maps as input or even include CNNs in an end-to-end DCV-based framework to generate the optimal AIF [22]. Related to this, there are methods that use CNNs with the sole purpose of directly estimating the perfusion maps, as such being able to overcome only some practical limitations of a DCV-based framework [46, 44, 89]. The use of native PWI or CTP as input is fairly new. Some methods use it as the sole input [88, 10], while most methods use it still in combination with other imaging such as DWI or the derived perfusion maps [83]. The latter approach, in combination with adversarial training, resulted in top-performing methods in the ISLES 2018 challenge [62, 19].

Incorporating metadata Putting pieces together, we know that apart from unleashing spatial context and model complexity on the imaging data, there is still non-imaging data, i.e. metadata, waiting impatiently to be incorporated. The dichotomization into reperfusers and non-reperfusers can be considered a naive way to incorporate the effects of the mTICI score and O24h, thereby producing two independent models that can deliver two virtual predictions, one for the core and one for the penumbra, respectively. This idea was similar to dichotomization based on IVT administration [79, 116]. However, for example, the TtT of each subject within each group differs, and this while the growth rate of the core has been shown to vary widely across different subjects [108, 39]. Similarly, recent DCV-based research has shown that there is a clear positive correlation between TtT and optimal rCBF threshold for core volume estimation [24]. Thus in general it would be interesting to incorporate more metadata in the model more naturally. In this respect, a first attempt was made to train a multi-variate generalized linear model that used both the CTP and clinical data to quantify the patient-specific dynamic change of tissue infarction depending on the TtT and mTICI score [54]. In a CNN-based setup, TsO, TtT, mTICI score and final recanalization status (O24h, i.e. is there an occlusion visible on ± 24 h follow-up imaging) were integrated beautifully and shown to have the desired effect [88, 115].

5 Conclusion

The brain hosts an intricate vasculature that is equipped with a variety of mechanisms to prevent ischemia. However, following an AIS the cerebral perfusion changes such that tissue becomes irreversibly or reversibly damaged, the core and the penumbra, respectively. Due to variability in defense mechanisms across different subjects and the complex interplay between time and location, the progression of the infarct is non-trivial. Either direct or indirect imaging methods can be used for patient triage to estimate the amount of salvageable tissue and assess the risk for potential complications. In clinical practice, the DCV-based triage via core-penumbra estimation still dominates. More specifically, thresholding of CTP-derived rCBF and Tmax maps for core and core \cup penumbra estimation, respectively. This is despite the fact that the research community has been able to complete the puzzle and came up with methods, e.g., using CNNs, that can incorporate the pathophysiology of AIS more naturally.

References

- [1] Diana Aguiar de Sousa, Rascha von Martial, Sònia Abilleira, ..., Valery Feigin, Valeria Caso, and Urs Fischer. Access to and delivery of acute ischaemic stroke treatments: A survey of national scientific societies and stroke experts in 44 European countries. *European Stroke Journal*, 4(1):13–28, March 2019.
- [2] Gregory W. Albers, Michael P. Marks, Stephanie Kemp, ..., Philip W Lavori, Joseph P Broderick, and Maarten G Lansberg. Thrombectomy for Stroke at 6 to 16 Hours with Selection by Perfusion Imaging. *New England Journal of Medicine*, 378(8):708–718, February 2018.
- [3] Gregory W. Albers, Vincent N. Thijs, Lawrence Wechsler, ..., Scott Hamilton, Michael Moseley, and Michael P. Marks. Magnetic resonance imaging profiles predict clinical response to early reperfusion: The diffusion and perfusion imaging evaluation for understanding stroke evolution (DEFUSE) study. *Annals of Neurology*, 60(5):508–517, November 2006.
- [4] J Astrup, B K Siesjö, and L Symon. Thresholds in cerebral ischemia - the ischemic penumbra. *Stroke*, 12(6):723–725, November 1981.
- [5] Oh Young Bang, Jeffrey L. Saver, Suk Jae Kim, ..., Bruce Ovbiagele, Kwang Ho Lee, and David S. Liebeskind. Collateral Flow Predicts Response to Endovascular Therapy for Acute Ischemic Stroke. *Stroke*, 42(3):693–699, March 2011.

- [6] Philip A Barber, Andrew M Demchuk, Jinjin Zhang, and Alastair M Buchan. Validity and reliability of a quantitative computed tomography score in predicting outcome of hyperacute stroke before thrombolytic therapy. *The Lancet*, 355(9216):1670–1674, May 2000.
- [7] J.C. Baron, M.G. Bousser, D. Comar, F. Soussaline, and P. Castaigne. Noninvasive Tomographic Study of Cerebral Blood Flow and Oxygen Metabolism in vivo. *European Neurology*, 20(3):273–284, 1981.
- [8] Jean-Claude Baron. Mapping the Ischaemic Penumbra with PET: Implications for Acute Stroke Treatment. *Cerebrovascular Diseases*, 9(4):193–201, 1999.
- [9] Olvert A. Berkhemer, Puck S.S. Fransen, Debbie Beumer, ..., Robert J. van Oostenbrugge, Charles B.L.M. Majoie, and Diederik W.J. Dippel. A Randomized Trial of Intraarterial Treatment for Acute Ischemic Stroke. *New England Journal of Medicine*, 372(1):11–20, January 2015.
- [10] Jeroen Bertels, David Robben, Dirk Vandermeulen, and Paul Suetens. Contra-Lateral Information CNN for Core Lesion Segmentation Based on Native CTP in Acute Stroke. In *LNCS*, volume 11383, pages 263–270. Springer Nature, 2019.
- [11] Andrew Bivard, Christopher Levi, Neil Spratt, and Mark Parsons. Perfusion CT in Acute Stroke: A Comprehensive Analysis of Infarct and Penumbra. *Radiology*, 267(2):543–550, May 2013.
- [12] Timothé Boutelier, Koshuke Kudo, Fabrice Pautot, and Makoto Sasaki. Bayesian Hemodynamic Parameter Estimation by Bolus Tracking Perfusion Weighted Imaging. *IEEE Transactions on Medical Imaging*, 31(7):1381–1395, July 2012.
- [13] Bruce C V Campbell, Henry Ma, Peter A Ringleb, ..., R. Burns, C. Johnston, and M. Williams. Extending thrombolysis to 4.5–9 h and wake-up stroke using perfusion imaging: a systematic review and meta-analysis of individual patient data. *The Lancet*, 394(10193):139–147, July 2019.
- [14] Bruce C.V. Campbell, Søren Christensen, Christopher R. Levi, ..., Geoffrey A. Donnan, Stephen M. Davis, and Mark W. Parsons. Cerebral blood flow is the optimal CT perfusion parameter for assessing infarct core. *Stroke*, 42(12):3435–3440, 2011.
- [15] Bruce C.V. Campbell, Peter J. Mitchell, Timothy J. Kleinig, ..., Patricia M. Desmond, Geoffrey A. Donnan, and Stephen M. Davis. Endovascular Therapy for Ischemic Stroke with Perfusion-Imaging Selection. *New England Journal of Medicine*, 372(11):1009–1018, March 2015.
- [16] Timothy J. Carroll, Sandra Horowitz, Wanyong Shin, ..., Saad Ali, Jeffrey Raizer, and Stephen Futterer. Quantification of cerebral perfusion using the “bookend technique”: an evaluation in CNS tumors. *Magnetic Resonance Imaging*, 26(10):1352–1359, December 2008.
- [17] José Castillo, Antoni Dávalos, and Manuel Noya. Progression of ischaemic stroke and excitotoxic aminoacids. *The Lancet*, 349(9045):79–82, January 1997.
- [18] Carlo W. Cereda, Søren Christensen, Bruce C.V. Campbell, ..., Gregory W. Albers, Mark W. Parsons, and Maarten G. Lansberg. A benchmarking tool to evaluate computer tomography perfusion infarct core predictions against a DWI standard. *Journal of Cerebral Blood Flow & Metabolism*, 36(10):1780–1789, October 2016.
- [19] Yu Chen, Yuexiang Li, and Yefeng Zheng. Ensembles of Modalities Fused Model for Ischemic Stroke Lesion Segmentation. In *LNCS*. Springer, 2019.
- [20] G.A. Christoforidis, C. Karakasis, Y. Mohammad, L.P. Caragine, M. Yang, and A.P. Slivka. Predictors of Hemorrhage Following Intra-Arterial Thrombolysis for Acute Ischemic Stroke: The Role of Pial Collateral Formation. *American Journal of Neuroradiology*, 30(1):165–170, January 2009.
- [21] Shelagh B. Coutts, Jessica E. Simon, Michael Eliasziw, ..., James N. Scott, Alastair M. Buchan, and Andrew M. Demchuk. Triaging transient ischemic attack and minor stroke patients using acute magnetic resonance imaging. *Annals of Neurology*, 57(6):848–854, June 2005.
- [22] Ezequiel de la Rosa, David Robben, Diana M. Sima, Jan S. Kirschke, and Bjoern Menze. Differentiable Deconvolution for Improved Stroke Perfusion Analysis. In *LNCS: MICCAI 2020*, pages 593–602. Springer International Publishing, 2020.
- [23] Gregory J del Zoppo and John M Hallenbeck. Advances in the Vascular Pathophysiology of Ischemic Stroke. *Thrombosis Research*, 98(3):73–81, May 2000.
- [24] Christopher D. D’Este, Mari E. Boesen, Seong Hwan Ahn, ..., Mayank Goyal, Ting Y. Lee, and Bijoy K. Menon. Time-Dependent Computed Tomographic Perfusion Thresholds for Patients With Acute Ischemic Stroke. *Stroke*, 46(12):3390–3397, December 2015.

- [25] F. Fahmi, H.A. Marquering, G.J. Streekstra, ..., B.K. Velthuis, E. VanBavel, and C.B. Majoie. Differences in CT Perfusion Summary Maps for Patients with Acute Ischemic Stroke Generated by 2 Software Packages. *American Journal of Neuroradiology*, 33(11):2074–2080, December 2012.
- [26] Behzad Farzin, Robert Fahed, Francois Guilbert, ..., Marc-Antoine Henry, Tim E Darsaut, and Jean Raymond. Early CT changes in patients admitted for thrombectomy. *Neurology*, 87(3):249–256, July 2016.
- [27] Andreas Fieselmann, Markus Kowarschik, Arundhuti Ganguly, Joachim Hornegger, and Rebecca Fahrig. Deconvolution-Based CT and MR Brain Perfusion Measurement: Theoretical Model Revisited and Practical Implementation Details. *International Journal of Biomedical Imaging*, 2011:1–20, 2011.
- [28] Alan Flores, Marta Rubiera, Marc Ribó, ..., Miguel Lemus, Pilar Coscojuela, and Carlos A. Molina. Poor Collateral Circulation Assessed by Multiphase Computed Tomographic Angiography Predicts Malignant Middle Cerebral Artery Evolution After Reperfusion Therapies. *Stroke*, 46(11):3149–3153, November 2015.
- [29] Jennifer E. Fugate and Alejandro A. Rabinstein. Absolute and Relative Contraindications to IV rt-PA for Acute Ischemic Stroke. *The Neurohospitalist*, 5(3):110–121, July 2015.
- [30] J H Garcia. Experimental ischemic stroke: a review. *Stroke*, 15(1):5–14, January 1984.
- [31] J H Garcia. Morphology of global cerebral ischemia. *Critical Care Medicine*, 16(10):979–987, October 1988.
- [32] J H Garcia, J B Hazelrig, H L Mitchem, ..., A G Hudetz, J H Halsey, and K A Conger. Transient Focal Ischemia in Subhuman Primates. *Journal of Neuropathology and Experimental Neurology*, 42(1):44–60, January 1983.
- [33] J H Garcia, Y Yoshida, H Chen, ..., J Lian, S Chen, and M Chopp. Progression from ischemic injury to infarct following middle cerebral artery occlusion in the rat. *The American journal of pathology*, 142(2):623–35, February 1993.
- [34] Julio H. Garcia, Kai-Feng Liu, and Khang-Loon Ho. Neuronal Necrosis After Middle Cerebral Artery Occlusion in Wistar Rats Progresses at Different Time Intervals in the Caudoputamen and the Cortex. *Stroke*, 26(4):636–643, April 1995.
- [35] Julio H. Garcia, Kai-Feng Liu, Zhu-Rong Ye, and Jorge A. Gutierrez. Incomplete Infarct and Delayed Neuronal Death After Transient Middle Cerebral Artery Occlusion in Rats. *Stroke*, 28(11):2303–2310, November 1997.
- [36] Mayank Goyal, Andrew M. Demchuk, Bijoy K. Menon, ..., Mark W. Lowerison, Tolulope T. Sajobi, and Michael D. Hill. Randomized Assessment of Rapid Endovascular Treatment of Ischemic Stroke. *New England Journal of Medicine*, 372(11):1019–1030, March 2015.
- [37] Mayank Goyal, Bijoy K Menon, Wim H van Zwam, ..., Jeffrey L Saver, Michael D Hill, and Tudor G Jovin. Endovascular thrombectomy after large-vessel ischaemic stroke: a meta-analysis of individual patient data from five randomised trials. *The Lancet*, 387(10029):1723–1731, April 2016.
- [38] Mayank Goyal, Johanna M. Ospel, Bijoy Menon, ..., Michael D. Hill, Diederik Dippel, and Marc Fisher. Challenging the Ischemic Core Concept in Acute Ischemic Stroke Imaging. *Stroke*, 51(10):3147–3155, October 2020.
- [39] Adrien Guenego, Michael Mlynash, Soren Christensen, ..., Jeremy J. Heit, Maarten G. Lansberg, and Gregory W. Albers. Hypoperfusion ratio predicts infarct growth during transfer for thrombectomy. *Annals of Neurology*, 84(4):616–620, October 2018.
- [40] Werner Hacke, Markku Kaste, Erich Bluhmki, ..., Rüdiger von Kummer, Nils Wahlgren, and Danilo Toni. Thrombolysis with Alteplase 3 to 4.5 Hours after Acute Ischemic Stroke. *New England Journal of Medicine*, 2008.
- [41] James Hampton-Till, Michael Harrison, Anna Luisa Kühn, ..., Eric Greveson, Michalis Papadakis, and Iris Q Grunwald. Automated Quantification of Stroke Damage on Brain Computed Tomography Scans: e-ASPECTS. *European Medical Journal of Neurology*, 3(1):69–74, 2015.
- [42] W.-D. Heiss and G. Rosner. Functional recovery of cortical neurons as related to degree and duration of ischemia. *Annals of Neurology*, 14(3):294–301, September 1983.
- [43] Christian Herweh, Peter A. Ringleb, Geraldine Rauch, ..., Daniel Richter, Simon Schieber, and Simon Nagel. Performance of e-ASPECTS software in comparison to that of stroke physicians on assessing CT scans of acute ischemic stroke patients. *International Journal of Stroke*, 11(4):438–445, June 2016.
- [44] Andreas Hess, Raphael Meier, Johannes Kaesmacher, ..., David Liebeskind, Roland Wiest, and Richard McKinley. Synthetic Perfusion Maps: Imaging Perfusion Deficits in DSC-MRI with Deep Learning. In *LNCS*, pages 447–455. Springer, 2019.
- [45] Randall T. Higashida and Anthony J. Furlan. Trial Design and Reporting Standards for Intra-Arterial Cerebral Thrombolysis for Acute Ischemic Stroke. *Stroke*, 34(8), August 2003.

- [46] King Chung Ho, Fabien Scalzo, Karthik V. Sarma, Suzie El-Saden, and Corey W. Arnold. A temporal deep learning approach for MR perfusion parameter estimation in stroke. In *2016 23rd International Conference on Pattern Recognition (ICPR)*, pages 1315–1320. IEEE, December 2016.
- [47] K-A. Hossmann. Viability thresholds and the penumbra of focal ischemia. *Annals of Neurology*, 36(4):557–565, October 1994.
- [48] K A Hossmann. Periarrest depolarizations. *Cerebrovascular and brain metabolism reviews*, 8(3):195–208, 1996.
- [49] Konstantin-Alexander Hossmann. Pathophysiology and Therapy of Experimental Stroke. *Cellular and Molecular Neurobiology*, 26(7-8):1055–1081, December 2006.
- [50] Georgios S. Ioannidis, Søren Christensen, Katerina Nikiforaki, ..., Mauricio Reyes, Maarten Lansberg, and Kostas Marias. Cerebral CT Perfusion in Acute Stroke: The Effect of Lowering the Tube Load and Sampling Rate on the Reproducibility of Parametric Maps. *Diagnostics*, 11(6):1121, June 2021.
- [51] U Ito, K Ohno, R Nakamura, F Sukanuma, and Y Inaba. Brain edema during ischemia and after restoration of blood flow. Measurement of water, sodium, potassium content and plasma protein permeability. *Stroke*, 10(5):542–547, September 1979.
- [52] Thomas H. Jones, Richard B. Morawetz, Robert M. Crowell, ..., Stuart J. FitzGibbon, Umberto DeGirolami, and Robert G. Ojemann. Thresholds of focal cerebral ischemia in awake monkeys. *Journal of Neurosurgery*, 54(6):773–782, June 1981.
- [53] Tudor G. Jovin, Angel Chamorro, Erik Cobo, ..., Rüdiger von Kummer, Miquel Gallofré, and Antoni Dávalos. Thrombectomy within 8 Hours after Symptom Onset in Ischemic Stroke. *New England Journal of Medicine*, 372(24):2296–2306, June 2015.
- [54] André Kemmling, Fabian Flottmann, Nils Daniel Forkert, ..., Marios Psychogios, Soenke Langner, and Jens Fiehler. Multivariate Dynamic Prediction of Ischemic Infarction and Tissue Salvage as a Function of Time and Degree of Recanalization. *Journal of Cerebral Blood Flow & Metabolism*, 35(9):1397–1405, September 2015.
- [55] Seymour S. Kety. Circulation and metabolism of the human brain in health and disease. *The American Journal of Medicine*, 8(2):205–217, February 1950.
- [56] Masatoshi Koga, Haruko Yamamoto, Manabu Inoue, ..., Kazumi Kimura, Kazuo Minematsu, and Kazunori Toyoda. Thrombolysis With Alteplase at 0.6 mg/kg for Stroke With Unknown Time of Onset. *Stroke*, 51(5):1530–1538, May 2020.
- [57] H. Kuang, M. Najm, D. Chakraborty, ..., A.M. Demchuk, B.K. Menon, and Wu Qiu. Automated ASPECTS on Noncontrast CT Scans in Patients with Acute Ischemic Stroke Using Machine Learning. *American Journal of Neuroradiology*, 40(1):33–38, January 2019.
- [58] T.-J. Lee and B. Murphy. Implementing Deconvolution Analysis for Perfusion CT. In *Multidetector Computed Tomography in Cerebrovascular Disease: CT Perfusion Imaging*, volume 29, pages e18–e19. Informa Healthcare, 4 edition, 2008.
- [59] David S. Liebeskind. Collateral Circulation. *Stroke*, 34(9):2279–2284, September 2003.
- [60] Longting Lin, Andrew Bivard, Venkatesh Krishnamurthy, Christopher R Levi, and Mark W Parsons. Whole-Brain CT Perfusion to Quantify Acute Ischemic Penumbra and Core. *Radiology*, 279(3):876–887, June 2016.
- [61] Weili Lin, Jin-Moo Lee, Yueh Z. Lee, Katie D. Vo, Thomas Pilgram, and Chung Y. Hsu. Temporal Relationship Between Apparent Diffusion Coefficient and Absolute Measurements of Cerebral Blood Flow in Acute Stroke Patients. *Stroke*, 34(1):64–70, January 2003.
- [62] Pengbo Liu. Stroke Lesion Segmentation with 2D Novel CNN Pipeline and Novel Loss Function. In *LNCS*, volume 11383, pages 253–262. Springer, 2019.
- [63] Cory Lorenz, Thomas Benner, Poe Jou Chen, ..., Yawu Liu, Juho Nuutinen, and A. Gregory Sorensen. Automated perfusion-weighted MRI using localized arterial input functions. *Journal of Magnetic Resonance Imaging*, 24:1133–1139, March 2006.
- [64] Christian Lucas, André Kemmling, Nassim Bouteldja, Linda F. Aulmann, Amir Madany Mamlouk, and Mattias P. Heinrich. Learning to Predict Ischemic Stroke Growth on Acute CT Perfusion Data by Interpolating Low-Dimensional Shape Representations. *Frontiers in Neurology*, 9(NOV):1–15, November 2018.
- [65] Henry Ma, Bruce C.V. Campbell, Mark W. Parsons, ..., Atte Meretoja, Stephen M. Davis, and Geoffrey A. Donnan. Thrombolysis Guided by Perfusion Imaging up to 9 Hours after Onset of Stroke. *New England Journal of Medicine*, 380(19):1795–1803, May 2019.

- [66] Matthew B. Maas, Michael H. Lev, Hakan Ay, ..., Andre Kemmling, Walter J. Koroshetz, and Karen L. Furie. Collateral Vessels on CT Angiography Predict Outcome in Acute Ischemic Stroke. *Stroke*, 40(9):3001–3005, September 2009.
- [67] Gilles Marchal, Vincent Beaudouin, Patrice Rioux, ..., Fausto Viader, Jean Michel Derlon, and Jean Claude Baron. Prolonged Persistence of Substantial Volumes of Potentially Viable Brain Tissue After Stroke. *Stroke*, 27(4):599–606, April 1996.
- [68] H. S. Markus. Cerebral perfusion and stroke. *Journal of Neurology, Neurosurgery & Psychiatry*, 75(3):353–361, March 2004.
- [69] J. R. Marler, T. Brott, P. Lyden, ..., E. C. Haley, M. Meyer, and B. C. Tilley. Tissue Plasminogen Activator for Acute Ischemic Stroke. *New England Journal of Medicine*, 333(24):1581–1588, December 1995.
- [70] Richard McKinley, Levin Häni, Jan Gralla, ..., Kaspar Mattmann, Mauricio Reyes, and Roland Wiest. Fully automated stroke tissue estimation using random forest classifiers (FASTER). *Journal of Cerebral Blood Flow & Metabolism*, 37(8):2728–2741, August 2017.
- [71] Ryan A. McTaggart, Tudor G. Jovin, Maarten G. Lansberg, ..., Manabu Inoue, Michael P. Marks, and Gregory W. Albers. Alberta Stroke Program Early Computed Tomographic Scoring Performance in a Series of Patients Undergoing Computed Tomography and MRI. *Stroke*, 46(2):407–412, February 2015.
- [72] Midas Meijis, Soren Christensen, Maarten G. Lansberg, Gregory W. Albers, and Fernando Calamante. Analysis of perfusion MRI in stroke: To deconvolve, or not to deconvolve. *Magnetic Resonance in Medicine*, 76(4):1282–1290, October 2016.
- [73] Bijoy K. Menon, Christopher D. D’Esterre, Emmad M. Qazi, ..., Leszek Hahn, Andrew M. Demchuk, and Mayank Goyal. Multiphase CT Angiography: A New Tool for the Imaging Triage of Patients with Acute Ischemic Stroke. *Radiology*, 275(2):510–520, May 2015.
- [74] Bijoy K Menon, Billy O’Brien, Andrew Bivard, ..., Xuewen Lu, Christopher Levi, and Mark W Parsons. Assessment of Leptomeningeal Collaterals Using Dynamic CT Angiography in Patients with Acute Ischemic Stroke. *Journal of Cerebral Blood Flow & Metabolism*, 33(3):365–371, March 2013.
- [75] Bijoy K. Menon, Eric E. Smith, Shelagh B. Coutts, ..., Hyuk-Won Chang, Jeong-Ho Hong, and Sung Il Sohn. Leptomeningeal collaterals are associated with modifiable metabolic risk factors. *Annals of Neurology*, 74(2):241–248, August 2013.
- [76] Sima Mraovitch and Richard Sercombe. *Neurophysiological Basis of Cerebral Blood Flow Control: An Introduction*. John Libbey & Co., 1 edition, 1996.
- [77] Simon Nagel, Devesh Sinha, Diana Day, ..., James Hampton-Till, Alastair M. Buchan, and Iris Q. Grunwald. e-ASPECTS software is non-inferior to neuroradiologists in applying the ASPECT score to computed tomography scans of acute ischemic stroke patients. *International Journal of Stroke*, 12(6):615–622, August 2017.
- [78] V. Nambiar, S. I. Sohn, M. A. Almekhlafi, ..., M. Goyal, M. D. Hill, and B. K. Menon. CTA Collateral Status and Response to Recanalization in Patients with Acute Ischemic Stroke. *American Journal of Neuroradiology*, 35(5):884–890, May 2014.
- [79] Anne Nielsen, Mikkel Bo Hansen, Anna Tietze, and Kim Mouridsen. Prediction of Tissue Outcome and Assessment of Treatment Effect in Acute Ischemic Stroke Using Deep Learning. *Stroke*, 49(6):1394–1401, June 2018.
- [80] Raul G. Nogueira, Ashutosh P. Jadhav, Diogo C. Haussen, ..., David S. Liebeskind, Jeffrey L. Saver, and Tudor G. Jovin. Thrombectomy 6 to 24 Hours after Stroke with a Mismatch between Deficit and Infarct. *New England Journal of Medicine*, 378(1):11–21, January 2018.
- [81] Jean Marc Olivot, Michael Mlynash, Vincent N. Thijs, ..., Roland Bammer, Michael P. Marks, and Gregory W. Albers. Optimal tmax threshold for predicting penumbral tissue in acute stroke. *Stroke*, 40(2):469–475, 2009.
- [82] J. H W Pexman, P. A. Barber, M. D. Hill, ..., M. E. Hudon, W. Y. Hu, and A. M. Buchan. Use of the Alberta Stroke Program Early CT Score (ASPECTS) for assessing CT scans in patients with acute stroke. *American Journal of Neuroradiology*, 22(8):1534–1542, 2001.
- [83] Adriano Pinto, Sérgio Pereira, Raphael Meier, ..., Roland Wiest, Carlos A. Silva, and Mauricio Reyes. Enhancing Clinical MRI Perfusion Maps with Data-Driven Maps of Complementary Nature for Lesion Outcome Prediction. In *MICCAI*, pages 107–115. Springer, 2018.
- [84] William J. Powers, Alejandro A. Rabinstein, Teri Ackerson, ..., Andrew M. Southerland, Deborah V. Summers, and David L. Tirschwell. 2018 Guidelines for the Early Management of Patients With Acute Ischemic Stroke: A Guideline for Healthcare Professionals From the American Heart Association/American Stroke Association. *Stroke*, 49(3), March 2018.

- [85] V. Puetz, I. Dzialowski, M. D. Hill, and A. M. Demchuk. The Alberta Stroke Program Early CT Score in Clinical Practice: What have We Learned? *International Journal of Stroke*, 4(5):354–364, October 2009.
- [86] Marc Ribo, Carlos A. Molina, Pilar Delgado, ..., Alex Rovira, Josep Munuera, and Jose Alvarez-Sabin. Hyperglycemia during Ischemia Rapidly Accelerates Brain Damage in Stroke Patients Treated with tPA. *Journal of Cerebral Blood Flow & Metabolism*, 27(9):1616–1622, September 2007.
- [87] Helena E. Riggs and Charles Rupp. Variation in Form of Circle of Willis. *Archives of Neurology*, 8(1):8, January 1963.
- [88] David Robben, Anna M.M. Boers, Henk A. Marquering, ..., Aad van der Lugt, Robin Lemmens, and Paul Suetens. Prediction of final infarct volume from native CT perfusion and treatment parameters using deep learning. *Medical Image Analysis*, 59:101589, January 2020.
- [89] David Robben and Paul Suetens. Perfusion Parameter Estimation Using Neural Networks and Data Augmentation. In *MICCAI-SWITCH workshop*, pages 439–446. Springer, 2019.
- [90] C. S. Roy and C. S. Sherrington. On the Regulation of the Blood-supply of the Brain. *The Journal of Physiology*, 11(1-2):85–158, January 1890.
- [91] Jeffrey L. Saver, Mayank Goyal, Alain Bonafe, ..., Richard du Mesnil de Rochemont, Oliver C. Singer, and Reza Jahan. Stent-Retriever Thrombectomy after Intravenous t-PA vs. t-PA Alone in Stroke. *New England Journal of Medicine*, 372(24):2285–2295, June 2015.
- [92] Fabien Scalzo, Qing Hao, Jeffry R. Alger, Xiao Hu, and David S. Liebeskind. Regional Prediction of Tissue Fate in Acute Ischemic Stroke. *Annals of Biomedical Engineering*, 40(10):2177–2187, October 2012.
- [93] Lauranne Scheldeman, Anke Wouters, and Robin Lemmens. Imaging selection for reperfusion therapy in acute ischemic stroke beyond the conventional time window. *Journal of Neurology*, 359:1317–1329, October 2021.
- [94] Sanjay K. Shetty and Michael H. Lev. CT Perfusion (CTP). In R. Gilberto González, Joshua A. Hirsch, W.J. Koroshetz, Michael H. Lev, and Pamela W. Schaefer, editors, *Acute Ischemic Stroke: Imaging and Intervention*, pages 87–113. Springer-Verlag, Berlin/Heidelberg, 2006.
- [95] J Marc Simard, Thomas A Kent, Mingkui Chen, Kirill V Tarasov, and Volodymyr Gerzanich. Brain oedema in focal ischaemia: molecular pathophysiology and theoretical implications. *The Lancet Neurology*, 6(3):258–268, March 2007.
- [96] S. Strandgaard, J. Olesen, E. Skinhoj, and N. A. Lassen. Autoregulation of Brain Circulation in Severe Arterial Hypertension. *BMJ*, 1(5852):507–510, March 1973.
- [97] L Symon, N M Branston, and O Chikovani. Ischemic brain edema following middle cerebral artery occlusion in baboons: relationship between regional cerebral water content and blood flow at 1 to 2 hours. *Stroke*, 10(2):184–191, March 1979.
- [98] I.Y.L. Tan, A.M. Demchuk, J. Hopyan, ..., S.P. Symons, A.J. Fox, and R.I. Aviv. CT Angiography Clot Burden Score and Collateral Score: Correlation with Clinical and Radiologic Outcomes in Acute Middle Cerebral Artery Infarct. *American Journal of Neuroradiology*, 30(3):525–531, March 2009.
- [99] Salwa El Tawil and Keith W Muir. Thrombolysis and thrombectomy for acute ischaemic stroke. *Clinical Medicine*, 17(2):161–165, April 2017.
- [100] Götz Thomalla, Florent Boutitie, Henry Ma, ..., Ona Wu, Albert J. Yoo, and Ramin Zand. Intravenous alteplase for stroke with unknown time of onset guided by advanced imaging: systematic review and meta-analysis of individual patient data. *The Lancet*, 396(10262):1574–1584, November 2020.
- [101] Götz Thomalla, Bastian Cheng, Martin Ebinger, ..., Jochen B. Fiebach, Jens Fiehler, and Christian Gerloff. DWI-FLAIR mismatch for the identification of patients with acute ischaemic stroke within 4-5 h of symptom onset (PRE-FLAIR): a multicentre observational study. *The Lancet Neurology*, 10(11):978–986, November 2011.
- [102] Götz Thomalla, Claus Z. Simonsen, Florent Boutitie, ..., Norbert Nighoghossian, Salvador Pedraza, and Christian Gerloff. MRI-Guided Thrombolysis for Stroke with Unknown Time of Onset. *New England Journal of Medicine*, 379(7):611–622, August 2018.
- [103] N V Todd, P Picozzi, A Crockard, and R W Russell. Duration of ischemia influences the development and resolution of ischemic brain edema. *Stroke*, 17(3):466–471, May 1986.
- [104] Henry M. Vander Eecken and Raymond D. Adams. The Anatomy and Functional Significance of the Meningeal Arterial Anastomoses of the Human Brain. *Journal of Neuropathology & Experimental Neurology*, 12(2):132–157, April 1953.

- [105] Nicolas Vila, Jose Castillo, Antonio Davalos, and Angel Chamorro. Proinflammatory Cytokines and Early Neurological Worsening in Ischemic Stroke. *Stroke*, 31(10):2325–2329, October 2000.
- [106] Rüdiger von Kummer and Imanuel Dzialowski. Imaging of cerebral ischemic edema and neuronal death. *Neuroradiology*, 59(6):545–553, June 2017.
- [107] Yang Wang, Weixing Hu, Alejandro D. Perez-Trepichio, ..., Anthony J. Furlan, Anthony W. Majors, and Stephen C. Jones. Brain Tissue Sodium Is a Ticking Clock Telling Time After Arterial Occlusion in Rat Focal Cerebral Ischemia. *Stroke*, 31(6):1386–1392, June 2000.
- [108] Hayley M. Wheeler, Michael Mlynash, Manabu Inoue, ..., Greg Zaharchuk, Matus Straka, and Gregory W. Albers. The Growth Rate of Early DWI Lesions is Highly Variable and Associated with Penumbra Salvage and Clinical Outcomes following Endovascular Reperfusion. *International Journal of Stroke*, 10(5):723–729, July 2015.
- [109] Richard P. White, Colin Deane, Patrick Vallance, and Hugh S. Markus. Nitric Oxide Synthase Inhibition in Humans Reduces Cerebral Blood Flow but Not the Hyperemic Response to Hypercapnia. *Stroke*, 29(2):467–472, February 1998.
- [110] Richard P. White, Claire Hindley, Peter M. Bloomfield, ..., Patrick Vallance, David J. Brooks, and Hugh S. Markus. The Effect of the Nitric Oxide Synthase Inhibitor L-NMMA on Basal CBF and Vasoneuronal Coupling in Man: A PET Study. *Journal of Cerebral Blood Flow & Metabolism*, 19(6):673–678, June 1999.
- [111] Max Wintermark, Adam E. Flanders, Birgitta Velthuis, ..., Julien Bogousslavsky, William P. Dillon, and Salvador Pedraza. Perfusion-CT Assessment of Infarct Core and Penumbra. *Stroke*, 37(4):979–985, April 2006.
- [112] Stefan Winzeck, Arsany Hakim, Richard McKinley, ..., Greg Zaharchuk, Roland Wiest, and Mauricio Reyes. ISLES 2016 and 2017-Benchmarking Ischemic Stroke Lesion Outcome Prediction Based on Multispectral MRI. *Frontiers in Neurology*, 9(SEP), September 2018.
- [113] R. J. S. Wise, S. Bernardi, R. S. J. Frackowiak, N. J. Legg, and T. Jones. Serial Observations on the Pathophysiology of Acute Stroke. *Brain*, 106(1):197–222, 1983.
- [114] Anke Wouters, Patrick Dupont, Soren Christensen, ..., Greg Albers, Vincent Thijs, and Robin Lemmens. Association Between Time From Stroke Onset and Fluid-Attenuated Inversion Recovery Lesion Intensity Is Modified by Status of Collateral Circulation. *Stroke*, 47(4):1018–1022, April 2016.
- [115] Anke Wouters, David Robben, Soren Christensen, ..., Gregory W. Albers, Paul Suetens, and Robin Lemmens. Prediction of Stroke Infarct Growth Rates by Baseline Perfusion Imaging. *Stroke*, 53(January), September 2021.
- [116] Ona Wu, Søren Christensen, Niels Hjort, ..., Götz Thomalla, Joachim Röther, and Leif Østergaard. Characterizing physiological heterogeneity of infarction risk in acute human ischaemic stroke using MRI. *Brain*, 129(9):2384–2393, September 2006.
- [117] Ona Wu, Walter J. Koroshetz, Leif Østergaard, ..., Lee H. Schwamm, Robert M. Weisskoff, and A. Gregory Sorensen. Predicting Tissue Outcome in Acute Human Cerebral Ischemia Using Combined Diffusion- and Perfusion-Weighted MR Imaging. *Stroke*, 32(4):933–942, April 2001.
- [118] Shadi Yaghi, Seena Dehkharghani, Eytan Raz, ..., Maarten G. Lansberg, Gregory W. Albers, and Adam de Havenon. The Effect of Hyperglycemia on Infarct Growth after Reperfusion: An Analysis of the DEFUSE 3 trial. *Journal of Stroke and Cerebrovascular Diseases*, 30(1), January 2021.
- [119] H Yonas, R P Pindzola, and D W Johnson. Xenon/computed tomography cerebral blood flow and its use in clinical management. *Neurosurgery clinics of North America*, 7(4):605–16, October 1996.